

# The Crystal Structure Study of $\text{CaSrFe}_{0.75}\text{Co}_{0.75}\text{Mn}_{0.5}\text{O}_{6-\delta}$ by Neutron Diffraction

Amara Martinson, Mandy Guinn, Ram Krishna Hona\*

Department of Environmental Science, United Tribes Technical College, Bismarck, USA

Email: \*rhona@uttc.edu

**How to cite this paper:** Martinson, A., Guinn, M. and Hona, R.K. (2024) The Crystal Structure Study of  $\text{CaSrFe}_{0.75}\text{Co}_{0.75}\text{Mn}_{0.5}\text{O}_{6-\delta}$  by Neutron Diffraction. *Journal of Materials Science and Chemical Engineering*, 12, 29-35.

<https://doi.org/10.4236/msce.2024.121003>

**Received:** December 10, 2023

**Accepted:** January 15, 2024

**Published:** January 18, 2024

Copyright © 2024 by author(s) and Scientific Research Publishing Inc. This work is licensed under the Creative Commons Attribution International License (CC BY 4.0).

<http://creativecommons.org/licenses/by/4.0/>



Open Access

## Abstract

The crystal structure of  $\text{CaSrFe}_{0.75}\text{Co}_{0.75}\text{Mn}_{0.5}\text{O}_{6-\delta}$  is investigated through neutron diffraction techniques in this study. The material is synthesized using a solid-state synthesis method at a temperature of 1200°C. Neutron diffraction data is subjected to Rietveld refinement, and a comparative analysis with X-ray diffraction (XRD) data is performed to unravel the structural details of the material. The findings reveal that the synthesized material exhibits a cubic crystal structure with a Pm-3m phase. The neutron diffraction results offer valuable insights into the arrangement of atoms within the lattice, contributing to a comprehensive understanding of the material's structural properties. This research enhances our knowledge of  $\text{CaSrFe}_{0.75}\text{Co}_{0.75}\text{Mn}_{0.5}\text{O}_{6-\delta}$ , with potential implications for its applications in various technological and scientific domains.

## Keywords

XRD, Neutron Diffraction, Perovskite Oxides, Crystal Structure, Solid-State Reaction

## 1. Introduction

Perovskite oxides exhibit a wide range of interesting and useful properties, such as ferroelectricity, [1] piezoelectricity, [2] superconductivity, [3] and catalytic activity. [4] [5] Due to these properties, perovskite oxides find applications in various fields, including electronics, catalysis, and energy storage. Perovskite oxides are recently the focus of research because of their potential applications in technology such as solid oxide fuel cells, [6] metal-air batteries, [7] Lithium battery, [8] electrocatalysis, [9] thermal insulation, [10] sensors, [11] and photovoltaics. [12] Oxygen plays an important role for the material to demonstrate a functional property, leading to exhibit excellent catalytic behavior in many tran-

sition-metal oxides. Perovskite-type systems, with the general formula  $ABO_3$ , are especially interesting, where A is usually an alkaline-earth metal or lanthanide, and B is usually a transition metal. The large A cations are located in spaces between corner-sharing  $BO_6$  octahedra.

It is possible to form oxide perovskite materials with some degree of oxygen deficiency. [13] In some cases, the vacant sites created due to oxygen deficiency can be distributed in the structure arbitrarily, forming a disordered system. One such material with a vacancy-disordered system is  $CaSrFe_{0.75}Co_{0.75}Mn_{0.5}O_{6-\delta}$ . [9] Among a series of compounds reported with different Mn concentrations in the composition  $CaSrFe_{1-x}Co_{1-x}Mn_{0.2x}O_{6-\delta}$ , the composition with  $x = 0.25$  demonstrated high efficiency of catalytic performance in oxygen generation and green hydrogen generation by water splitting.

Structural properties are the backbone for the functional properties and efficiency of material toward any application performance. So, scientists generally study in depth the structural properties of a material that illustrates outstanding performance with a better functional property. Since  $CaSrFe_{0.75}Co_{0.75}Mn_{0.5}O_{6-\delta}$  outperformed the electrocatalytic behavior of water splitting for oxygen and hydrogen production, we are interested in studying its crystal structure by neutron diffraction.  $CaSrFe_{0.75}Co_{0.75}Mn_{0.5}O_{6-\delta}$  has been reported for its structural analysis by powder XRD, SEM and XPS. However, its structural analysis has not been reported by powder neutron diffraction which can support the previously reported structural data of XRD for this material.

## 2. Experimental

$CaSrFe_{0.75}Co_{0.75}Mn_{0.5}O_{6-\delta}$  was synthesized by solid state reaction method at high temperatures by mixing stoichiometric amount of  $CaCO_3$ ,  $SrCO_3$ ,  $Fe_2O_3$ ,  $Co_3O_4$  and  $Mn_2O_3$ . The precursor chemicals were mixed uniformly in agate mortar and pestle. The mixture is pelletized using pellet die and a hydraulic pressure at a pressure of 3 tons. The dimensions of the cylindrical pellets were 2 - 3 mm thick with a diameter of 10 mm. They were fired at  $1000^\circ C$  in the air in a muffle furnace for 12 hours. The heating and cooling rate was 5 degrees per minute. Once the pellet was cooled down, it was powdered and repelletized which was followed by a second firing at  $1200^\circ C$ . It was heated at  $1200^\circ C$  for 24 hours. This time the heating and cooling ramp was maintained at a rate of 100 degrees per hour. The cold pellet was powdered which was subjected to phase purity and structure of the polycrystalline samples were determined by powder X-ray diffraction (XRD) [14] at room temperature using  $Cu K\alpha 1$  radiation ( $\lambda = 1.54056 \text{ \AA}$ ) using Bruker phaser D2 diffractometer and neutron diffraction at room temperature. The GSAS software [15] and EXPEGUI [16] interface were used for Rietveld refinements.

## 3. Results and Discussion

$CaSrFe_{0.75}Co_{0.75}Mn_{0.5}O_{6-\delta}$  is an oxygen deficient cubic perovskite oxide. It has

$Pm-3m$  space group. Its XRD data and Rietveld refined cell parameters are shown in **Figure 1** and **Table 1**, respectively. The results are in agreement with the previous report. [9] The crystal structure and its neutron diffraction data are shown in **Figure 2** and **Figure 3**, respectively. Neutron diffraction data also shows the cubic structure with  $Pm-3m$  space group in agreement with the XRD data. Its refined cell parameters are shown in **Table 2**. As mentioned in introduction, oxygen deficient perovskites are represented by a general formula  $ABO_{3-\delta}$  or  $A_2B_2O_{6-\delta}$  where A is alkaline earth metal and B is 3d or 4d transition metal. In our material  $CaSrFe_{0.75}Co_{0.75}Mn_{0.5}O_{6-\delta}$ , A site is occupied by Ca and Sr and B site is occupied by Fe, Co and Mn.

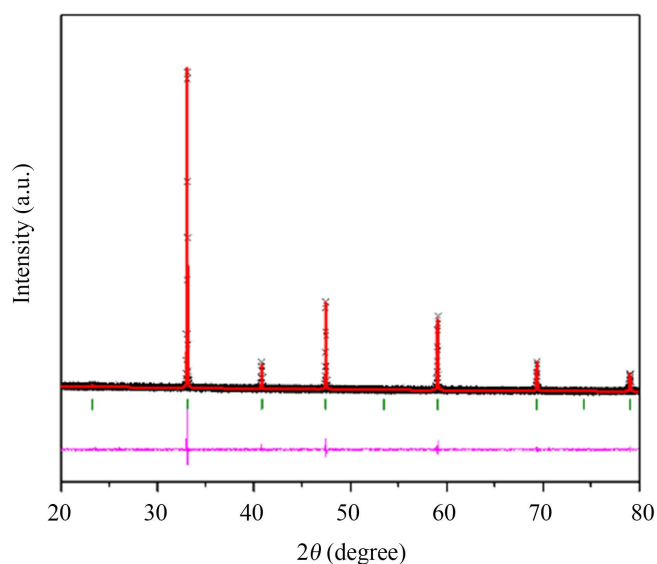


**Figure 1.** Rietveld refinement profile for powder XRD data refined in the space group  $Pm-3m$ . Crosses represent experimental data, the solid red line is the model, vertical green tick marks show Bragg peak positions, and the lower pink line represents the difference plot.

**Table 1.** The unit cell parameters and Powder X-ray data refinement profile for  $CaSrFe_{0.75}Co_{0.75}Mn_{0.5}O_{6-\delta}$ .

Space group	Cell volume ( $\text{\AA}^3$ )	A ( $\text{\AA}$ )	Angles	WRp	Rp	
$Pm-3m$	56.092 (8)	3.82795 (6)	$90^\circ$	0.0423	0.0322	
Elements	$x$	$y$	$z$	Multiplicity	Occupancy	Uiso
Ca	0.5	0.5	0.5	1	0.5	0.0269 (2)
Sr	0.5	0.5	0.5	1	0.5	0.0269 (2)
Fe	0.0	0.0	0.0	1	0.375	0.0439 (8)
Mn	0.0	0.0	0.0	1	0.250	0.0439 (8)
Co	0.0	0.0	0.0	1	0.375	0.0439 (8)
O	0.5	0.0	0.0	3	0.8533	0.0599 (4)

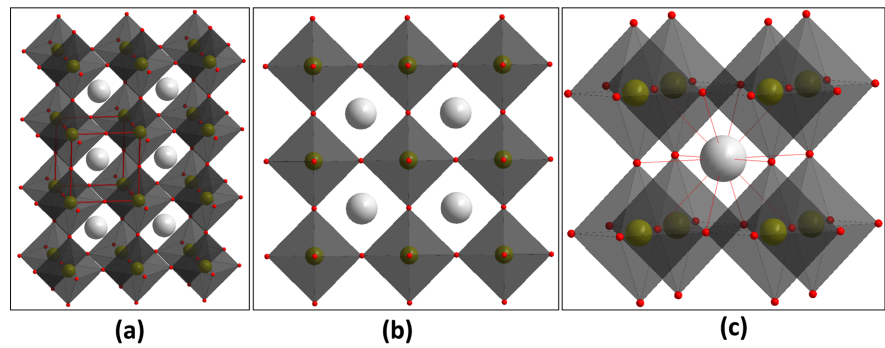


**Figure 2.** Crystal structure (a) Crystallographic unit cell and corner-sharing (Fe/Co/Mn)O<sub>6</sub> octahedra (black) are highlighted. The large white-gray spheres are the Ca and Sr atoms. (b) View along the unit cell axis. Because of the cubic symmetry, the three axes are identical. (c) Coordination geometry around the Ca/Sr atom, which is 12-coordinated.

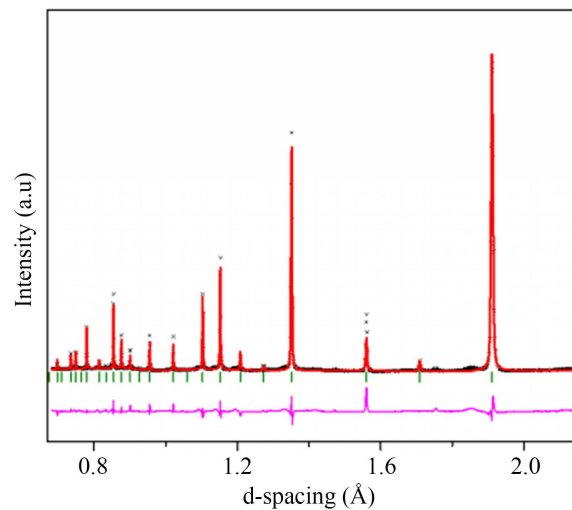


**Figure 3.** Neutron diffraction Rietveld refinement profile. Crosses represent experimental data, the solid red line is the *Pm-3m* model, vertical green tick marks show Bragg peak positions, and the lower pink line represents the difference plot.

**Table 2.** The unit cell parameters and powder neutron diffraction data refinement profile for CaSrFe<sub>0.75</sub>Co<sub>0.75</sub>Mn<sub>0.5</sub>O<sub>6-δ</sub>.

Space group	Cell volume (Å <sup>3</sup> )	A (Å)	Angles	wRp	Rp	
<i>Pm-3m</i>	55.774 (4)	3.8207 (1)	90°	0.0993	0.1061	
Elements	x	y	z	Multiplicity	Occupancy	Uiso
Ca	0.5	0.5	0.5	1	0.5	0.0117 (6)
Sr	0.5	0.5	0.5	1	0.5	0.0117 (4)
Fe	0.0	0.0	0.0	1	0.375	0.0095 (5)
Mn	0.0	0.0	0.0	1	0.250	0.0095 (5)
Co	0.0	0.0	0.0	1	0.375	0.0095 (5)
O	0.5	0.0	0.0	3	0.8533	0.0323 (8)

**Table 3.** Comparison of the bond lengths (Å) between neutron diffraction and powder X-ray diffraction data.

Neutron	XRD
Ca-O 2.70146 (3)	Ca-O 2.70680 (2)
Sr-O 2.70146 (3)	Sr-O 2.70680 (2)
Fe-O 1.91022 (3)	Fe-O 1.91399 (2)
Co-O 1.91022 (3)	Co-O 1.91399 (2)
Mn-O 1.91022 (3)	Mn-O 1.91399 (2)

If we closely look at **Figure 2**, it can be seen that the Fe/Co/Mn atoms (seen as green spheres) are surrounded by 6 oxygen atoms (small red spheres) in octahedral positions. Here, imaginary planes (black planes) are drawn connecting oxygen atoms to make the octahedral structures clear. It can be represented as  $\text{BO}_6$  octahedra. So, Fe/Co/Mn atoms are 6 coordinated throughout the crystal lattice as shown in **Figure 2(a)** except at the oxygen deficient positions (which are not shown due to uncertainty). Since the composition is  $\text{CaSrFe}_{0.75}\text{Co}_{0.75}\text{Mn}_{0.5}\text{O}_{6-\delta}$  Fe and Co occupy 75% of the B site positions, each occupying 37.5% of the total B site positions and Mn occupies 25% of the B-site positions. It can be seen in **Figure 2(c)** that the whitish grey largest sphere, which is Ca/Sr atom, is surrounded by 8 octahedra. Ca and Sr share equally the A-site positions, each occupying 50% of the A-sites. Ca/Sr is 12 coordinated except at the oxygen deficient positions (which are not shown due to uncertainty). The octahedra are connected to one another by corner sharing through oxygen. Thus, the bonding pattern is B-O-B where B is Fe/Co/Mn. The B-O-B bond angle is  $180^\circ$ . The B-O-B bonds lengths are shown in **Table 2** and **Table 3** for XRD and Neutron diffraction.

#### 4. Conclusion

A perovskite material with a composition of  $\text{CaSrFe}_{0.75}\text{Co}_{0.75}\text{Mn}_{0.5}\text{O}_{6-\delta}$  was synthesized by solid-state reaction at 1200 C. Its crystal structure was investigated by neutron diffraction and compared with that of XRD data. Neutron data revealed its structure cubic with the  $Pm-3m$  phase which supported the XRD data. The study showed that the B cations are surrounded by 6 oxygens forming  $\text{BO}_6$  octahedra which are interconnected by corner sharing through O-atoms and A cations are surrounded by 8 such octahedra.

#### Acknowledgements

This work is supported in part by the National Science Foundation Tribal College and University Program Instructional Capacity Excellence in TCUP Institutions (ICE-TI) award # 1561004. A part of this work is also supported by NSF grant No. HRD 1839895. Additional support for the work came from ND EPSCOR STEM grants for the purchase of potentiostat and X-ray diffractometer. Permission

was granted by United Tribes Technical Colleges (UTTC) Environmental Science Department to publish this information. The views expressed are those of the authors and do not necessarily represent those of United Tribes Technical College.

### Funding

Instructional Capacity Excellence in TCUP Institutions (ICE-TI) award #1561004 and NSF Tribal Enterprise Advancement Center award grant No. HRD 1839895.

### Institutional Review Board Statement

Not Applicable.

### Informed Consent Statement

Not applicable.

### Conflicts of Interest

The authors declare no conflict of interest.

### References

- [1] Cohen, R.E. (1992) Origin of Ferroelectricity in Perovskite Oxides. *Nature*, **358**, 136-138. <https://doi.org/10.1038/358136a0>
- [2] Tyunina, M. (2020) Oxygen Vacancies in Perovskite Oxide Piezoelectrics. *Materials*, **13**, 5596. <https://doi.org/10.3390/ma13245596>
- [3] Kim, M., McNally, G.M., Kim, H.-H., Oudah, M., Gibbs, A.S., Manuel, P., *et al.* (2022) Superconductivity in (Ba,K)SbO<sub>3</sub>. *Nature Mater*, **21**, 627-633. <https://doi.org/10.1038/s41563-022-01203-7>
- [4] Hona, R.K. and Ramezanipour, F. (2019) Remarkable Oxygen-Evolution Activity of a Perovskite Oxide from the Ca<sub>2-x</sub>Sr<sub>x</sub>Fe<sub>2</sub>O<sub>6-δ</sub> Series. *Angewandte Chemie International Edition*, **58**, 2060-2063. <https://doi.org/10.1002/anie.201813000>
- [5] Hona, R.K., Karki, S.B. and Ramezanipour, F. (2020) Oxide Electrocatalysts Based on Earth-Abundant Metals for Both Hydrogen—And Oxygen-Evolution Reactions. *ACS Sustainable Chemistry & Engineering*, **8**, 11549-11557. <https://doi.org/10.1021/acssuschemeng.0c02498>
- [6] Shu, L., Sunarso, J., Hashim, S.S., Mao, J., Zhou, W., *et al.* (2019) Advanced Perovskite Anodes for Solid Oxide Fuel Cells: A Review. *International Journal of Hydrogen Energy*, **44**, 31275-31304. <https://doi.org/10.1016/j.ijhydene.2019.09.220>
- [7] Takeguchi, T., Yamanaka, T., Takahashi, H., Watanabe, H., Kuroki, T., *et al.* (2013) Layered Perovskite Oxide: A Reversible Air Electrode for Oxygen Evolution/Reduction in Rechargeable Metal-Air Batteries. *Journal of the American Chemical Society*, **135**, 11125-11130. <https://doi.org/10.1021/ja403476v>
- [8] Hona, R.K., Thapa, A.K., Ramezanipour, F. (2020) An Anode Material for Lithium-Ion Batteries Based on Oxygen-Deficient Perovskite Sr<sub>2</sub>Fe<sub>2</sub>O<sub>6-δ</sub>. *Chemistry-Select*, **5**, 5706-5711. <https://doi.org/10.1002/slct.202000987>
- [9] Hona, R.K., Karki, S.B., Cao, T., Mishra, R., Sterbinsky, G.E. and Ramezanipour, F. (2021) Sustainable Oxide Electrocatalyst for Hydrogen- and Oxygen-Evolution Reactions. *ACS Catalysis*, **11**, 14605-14614. <https://doi.org/10.1021/acscatal.1c03196>
- [10] Hona, R.K., Karki, S.B., Dhaliwal, G., Guinn, M. and Ramezanipour, F. (2022) High

- Thermal Insulation Properties of  $A_2FeCoO_{6-\delta}$  ( $A = Ca, Sr$ ). *Journal of Materials Chemistry C*, **10**, 12569-12573. <https://doi.org/10.1039/D2TC03007A>
- [11] Karki, S.B., Hona, R.K. and Ramezanipour, F. (2020) Effect of Structure on Sensor Properties of Oxygen-Deficient Perovskites,  $A_2BB'O_5$  ( $A = Ca, Sr$ ;  $B = Fe$ ;  $B' = Fe, Mn$ ) for Oxygen, Carbon Dioxide and Carbon Monoxide Sensing. *Journal of Electronic Materials*, **49**, 1557-1567. <https://doi.org/10.1007/s11664-019-07862-8>
- [12] Kumar, A. (2021) Oxide Perovskites and Their Derivatives for Photovoltaics Applications. In: Kumar, A., Ed., *Advanced Ceramics for Energy and Environmental Applications*, 1st Edition, CRC Press, Boca Raton, 15.
- [13] Sanchez, S.N., Guinn, M., Phuyal, U.S., Dhaliwal, G.S. and Hona, R.K. (2023) Specific Heat Capacity of  $A_2FeCoO_{6-\delta}$  ( $A = Ca$  or  $Sr$ ). *Journal of Materials Science and Chemical Engineering*, **11**, 1-10.
- [14] Hona, R.K., Guinn, M., Phuyal, U.S., Sanchez, S.N. and Dhaliwal, G.S. (2023) Alkali Ionic Conductivity in Inorganic Glassy Electrolytes. *Journal of Materials Science and Chemical Engineering*, **11**, 31-72. <https://doi.org/10.4236/msce.2023.117004>
- [15] Toby, B.H. and Von Dreele, R.B. (2013) GSAS-II: The Genesis of a Modern Open-Source All Purpose Crystallography Software Package. *Journal of Applied Crystallography*, **46**, 544-549. <https://doi.org/10.1107/S0021889813003531>
- [16] Toby, B.H. (2001) EXPGUI, A Graphical User Interface for GSAS. *Journal of Applied Crystallography*, **34**, 210-213. <https://doi.org/10.1107/S0021889801002242>